

Simulating full-waveform LIDAR

Angela M. Kim^{*}, Richard C. Olsen, Carlos F. Borges
Naval Postgraduate School, 1 University Circle, Monterey, CA 93943

ABSTRACT

A simple Monte Carlo model of laser propagation through a tree is presented which allows the simulation of full-waveform LIDAR signatures. The model incorporates a LIDAR system and a 'natural' scene, including an atmosphere, tree and ground surface. The PROSPECT leaf reflectance model is incorporated to determine leaf radiometric properties. Changes in the scene such as varying material reflectance properties, sloped vs. flat ground, and comparisons of tree 'leaf-on' vs. 'leaf-off' conditions have been analyzed. Changes in the LIDAR system have also been studied, including the effects of changing laser wavelength, shape and length of transmitted pulses, and angle of transmission. Results of some of these simulations are presented.

Keywords: LIDAR model, Monte Carlo simulation, PROSPECT Leaf Reflectance model, full-waveform

INTRODUCTION

The motivation for developing this LIDAR simulation capability is to enable research of the factors that influence the shape of LIDAR waveforms, and to assist in the development of waveform processing algorithms. The model presented here incorporates a LIDAR system and a 'natural' scene, including an atmosphere, tree and ground surface. A simple Monte Carlo method is used to simulate laser propagation and waveform creation.

Results from a series of test cases are presented which illuminate various aspects of the model. These test cases illustrate the effects of changing the number of model iterations, LIDAR system sampling frequency, varying material reflectance properties, and varying LIDAR pulse length and angular beam spread. Test cases with varying levels of scene complexity demonstrate the effects of physical changes in the scene on the recorded waveform, and illustrate the difficulty of full-waveform LIDAR analysis.

1. THE MODEL

1.1 The LIDAR System

The simulated LIDAR system has variable transmission and receiver parameters, including initial pulse energy, pulse shape and length, minimum detection energy, angular beam spread, sensor aperture size, sensor flying height and location, timing accuracy, and laser wavelength. Table 1 lists some of the default model settings. The effects of varying some of these parameters are illustrated in the Test Cases section of this paper.

Table 1. LIDAR system parameters and settings.

LIDAR System Parameters	
Flying altitude above ground	1000 m
Pulse width	6 ns
Laser wavelength	1064 nm
Beam divergence	0.3 mrad
Aperture of receiving optics	0.2 m
Laser pointing angle (degrees from nadir)	0°

* amkim@nps.edu; phone 1 831 656-3330; fax 1 831 656-2834

1.2 The Tree

A simulated tree was created to study the LIDAR waveform of complex scenes. The tree model consists of two components: the physical shape and arrangement of branches, twigs and leaves, and the reflectance properties of these materials. The shape of the tree is modeled based on a method called Lindenmayer-systems, or L-systems for short, which were developed by Aristid Lindenmayer in 1968 to study the geometric growth patterns of plants (Prusinkiewicz, 2004). The tree used in the simulations for this paper is illustrated with and without leaves in Figure 1. The physical parameters of the tree can be adjusted as desired. The default settings used in the test cases presented in this paper are shown in Table 2.

Tree bark and ground surface radiometric values are assigned based on spectra taken from the U.S. Geological Survey (USGS) vegetation library (Clark, 1993). Leaf radiometric values were determined using the PROSPECT leaf reflectance model.

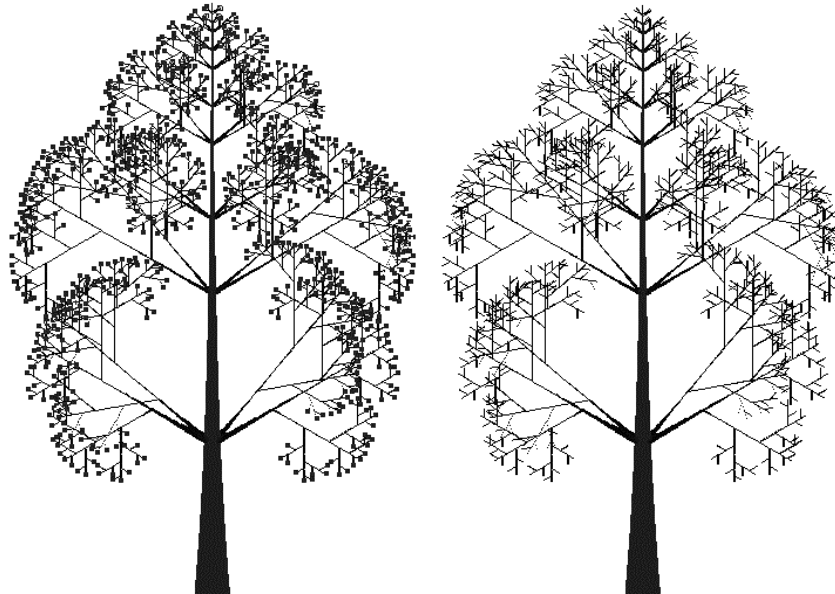


Figure 1. L-System tree model output; tree with and without leaves.

Table 2. Physical units of L-System tree.

Tree Parameters	
Tree height	15 m
Tree trunk width at base	0.89 m
Smallest branches modeled	0.03 m
Leaf clump diameter	0.06 m

Within the tree, bud locations are designated for each leaf, and a defined shape or radius around each bud is defined as containing leaves. This radius can be adjusted to simulate more (or less) leaf coverage. The bark and leaf models are combined as a probability map, with each location assigned a likelihood of being bark, leaf, or air.

1.3 The Leaves

Leaf reflectance, transmission, and absorption values are determined according to the PROSPECT leaf reflectance model of Jacquemoud and Baret (Jacquemoud, 1990). PROSPECT is a radiative transfer model that models a leaf as a series of plates. Multiple studies have validated PROSPECT as a leaf optical properties model. The PROSPECT model incorporates a number of physical parameters that determine leaf reflectance. The default values for initializing the model are shown in Table 3. These default settings produce a vegetation spectrum as illustrated in Figure 2. The spectra were sampled at the selected laser wavelength to determine the leaf radiometric properties for the LIDAR simulation.

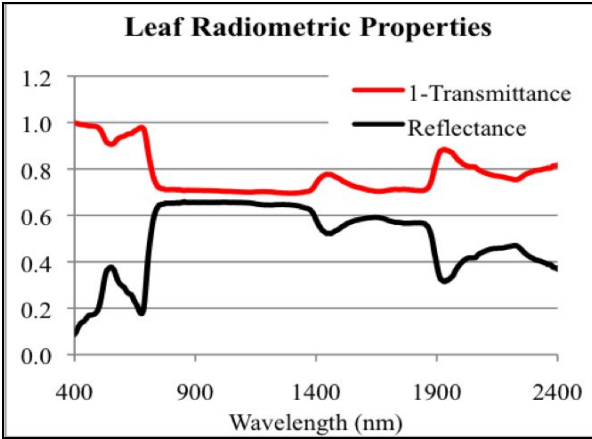


Figure 2. Leaf radiometric properties as determined by the PROSPECT leaf reflectance model.

Table 3. Parameters and settings used to simulate the leaf reflectance spectra using PROSPECT v2.01.

PROSPECT v2.01 Parameters	
Leaf equivalent thickness (n)	3.4
Chlorophyll a+b (cab)	20.0
Water (cw)	0.002
Protein (cp)	0.001
Structural biochemicals (cc)	0.001
Leaf angle (deg)	0°

1.4 LIDAR Propagation and Waveform Creation

The propagation of the LIDAR pulses and the creation of the waveform is accomplished using a Monte Carlo approach. Multiple LIDAR pulses are propagated through the system, and the average response is output as the simulated waveform. Each LIDAR pulse is defined as having a certain length, energy level, and beam divergence. The pulse is divided into multiple short time bins, with each bin being treated as a separate pulse having an initial energy, location and propagation direction determined by its location in time in the LIDAR pulse. The initial start time is adjusted based on the bin location; for a 6 ns pulse, the initial bin pulse will be transmitted at time 0, while the last bin will be transmitted just prior to 6 ns.

Each pulse bin is propagated with a user-defined step size. At each step, the location of the LIDAR pulse is tracked, and the material interaction is determined probabilistically according to the material probability maps, and reflectance properties. When the pulse interacts with material having an absorbance greater than 0, the energy of the pulse is reduced by that amount. The remaining energy is allowed to continue propagating. If the energy is transmitted, the angle of propagation is not changed. If the energy is reflected, the angle of propagation is updated.

Reflection can be either Lambertian or specular. If the reflection is Lambertian, every angle of reflection between 0 and π radians from the material surface is equally likely, so an angle of reflection in this range is chosen randomly. In the specular case, the reflection is assumed to be a mirrored reflection from the plane of the material being impacted. Figure 3 illustrates the difference between reflections from a specular and Lambertian surface.

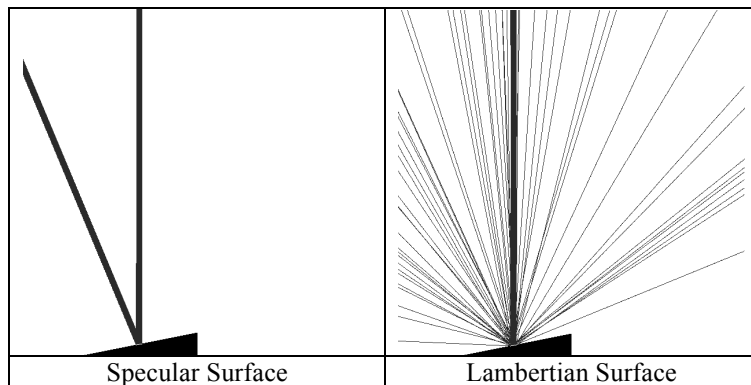


Figure 3. Interaction of a pulse of LIDAR energy, with the surface modeled as being a specular surface and as a Lambertian surface.

Each pulse bin of energy is tracked until the energy is returned to the sensor, scattered out of the workspace and lost, or absorbed by materials within the scene. Some of the pulse bins may have an initial energy level below the detection level of the LIDAR system—this energy is considered lost. There is an option within the LIDAR propagation model to set a maximum number of allowed scattering events; if a pulse interacts more times than allowed, the energy is considered lost. If the energy is returned to the sensor, the time-of-flight and the amount of energy is recorded. This process is repeated for each pulse bin. Returns occurring at exactly the same time are averaged, and a waveform is created for each pulse. This process is repeated for multiple pulses, and the waveforms are averaged to create the simulated waveform. The waveform is resampled so that the total energy contained in the waveform matches the amount of energy returned to the sensor.

2. TEST CASES

A series of test cases are presented which demonstrate different aspects of the model. The LIDAR model was initiated with the LIDAR system parameters as shown in Table 1, except as where otherwise noted. Physical parameters for the tree model are listed in Table 2.

2.1 Test Case 1 – Varying Number of Model Iterations and LIDAR System Sampling Frequency

The number of iterations necessary to accurately simulate the waveform depends upon the complexity of the scene. The number of necessary iterations can be determined automatically by setting a threshold for the amount of new information being added to the waveform after each iteration.

When looking at a very simple situation, such as a flat surface with no obstructions, very few pulses are needed to accurately simulate the LIDAR waveform. As an illustration, a flat Lambertian surface is simulated (Figure 4). In Figure 5, the amount of new information being added to the waveform as the number of model iterations increases is shown to level off fairly quickly for this non-complex scene.

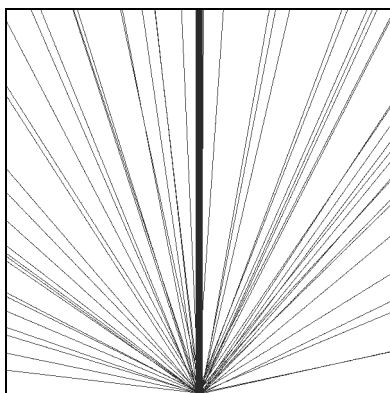


Figure 4. Interaction of LIDAR pulse with a flat Lambertian surface.

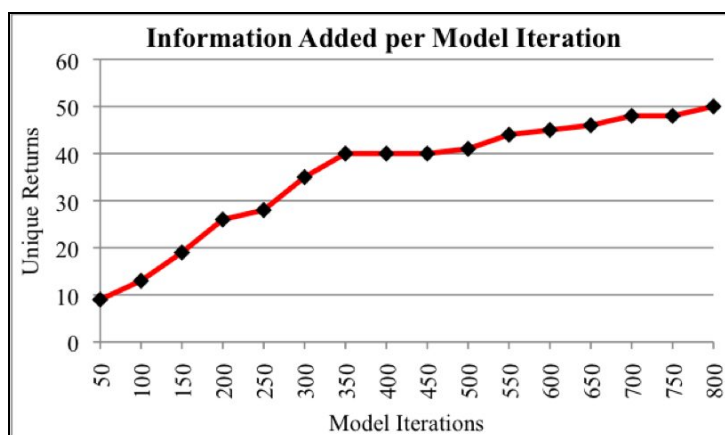


Figure 5. Number of unique returns added to the simulated waveform as a function of the number of model iterations.

Increasing the number of model iterations causes the waveform to become smoother and more complete. As shown in Figure 6, after only 100 iterations, the waveform peak can be correctly detected. As more iterations are completed, the simulated waveform becomes smoother.

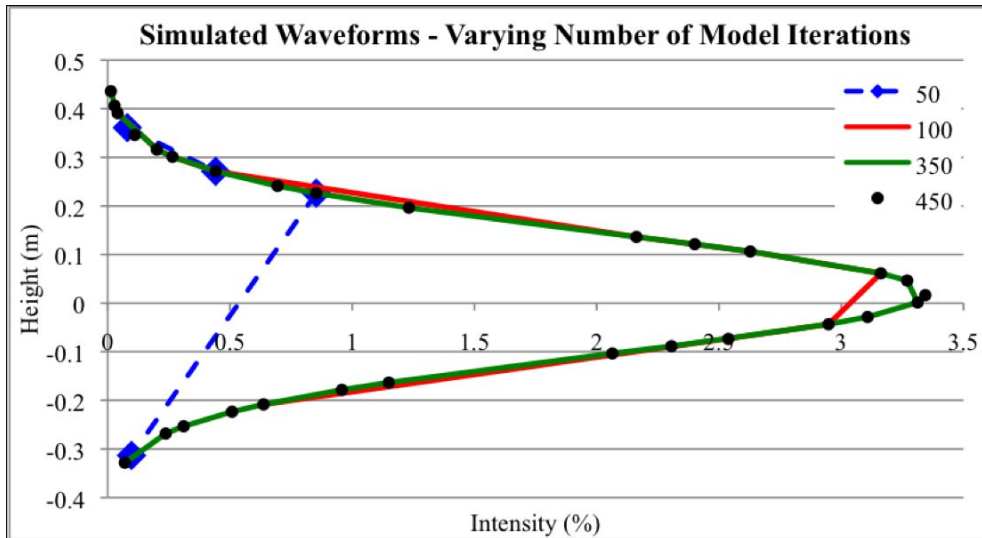


Figure 6. Simulated LIDAR waveform from a flat Lambertian surface after varying numbers of model iterations.

As the complexity of the scene increases, more pulses must be simulated to accurately capture the waveform detail. A complex scene incorporating a tree with leaves is shown in Figure 7, along with associated heights and the interaction of the first pulse of LIDAR energy.

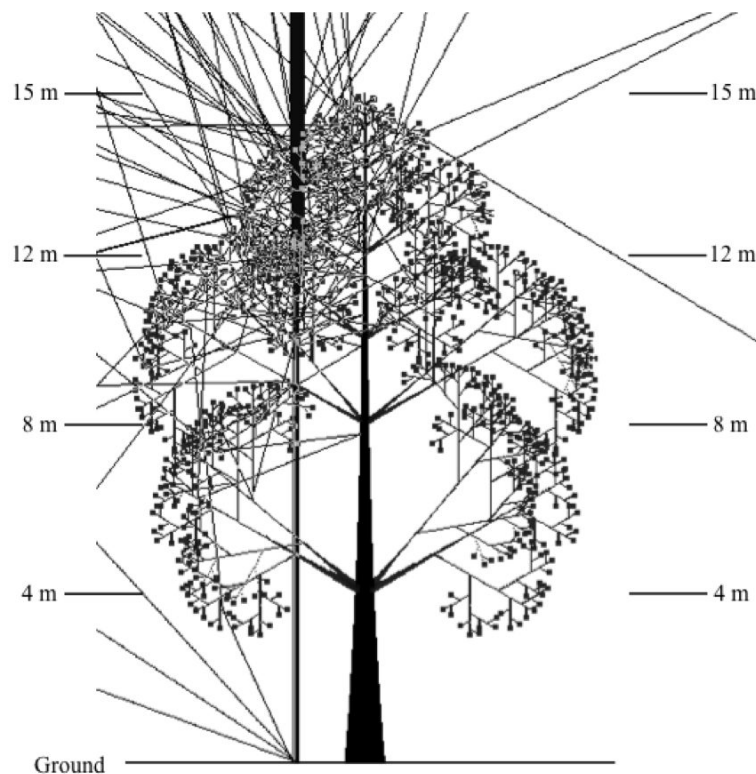


Figure 7. Interaction of first pulse of LIDAR energy.

For this complex scene, nearly 1.5 million iterations are needed before the simulated waveform starts to stabilize (Figure 8).

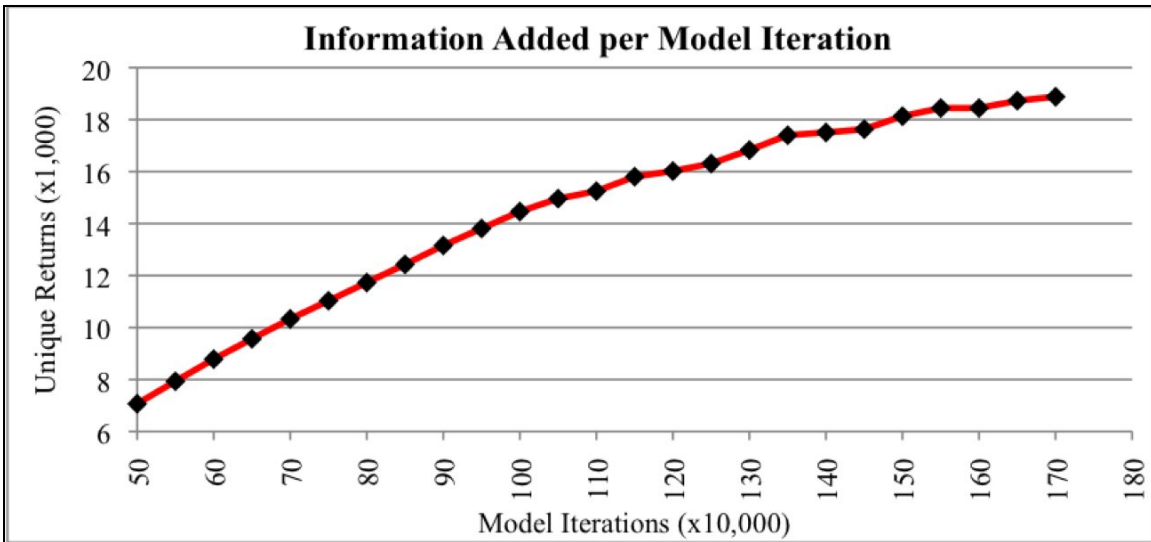


Figure 8. Number of unique returns added to the simulated waveform as a function of the number of model iterations.

The waveform recorded by a LIDAR system depends on the sampling frequency of the sensor. As the sampling frequency increases, more detail is recorded, and a higher level of accuracy is maintained.

The waveform created from this simulation, and the effect of increasing the LIDAR system sampling frequency, is shown in Figure 9. Sampling is accomplished by creating time bins starting with the time at which the initial energy returns to the sensor. This creates an artifact in the waveform where the ground peak appears higher than it should.

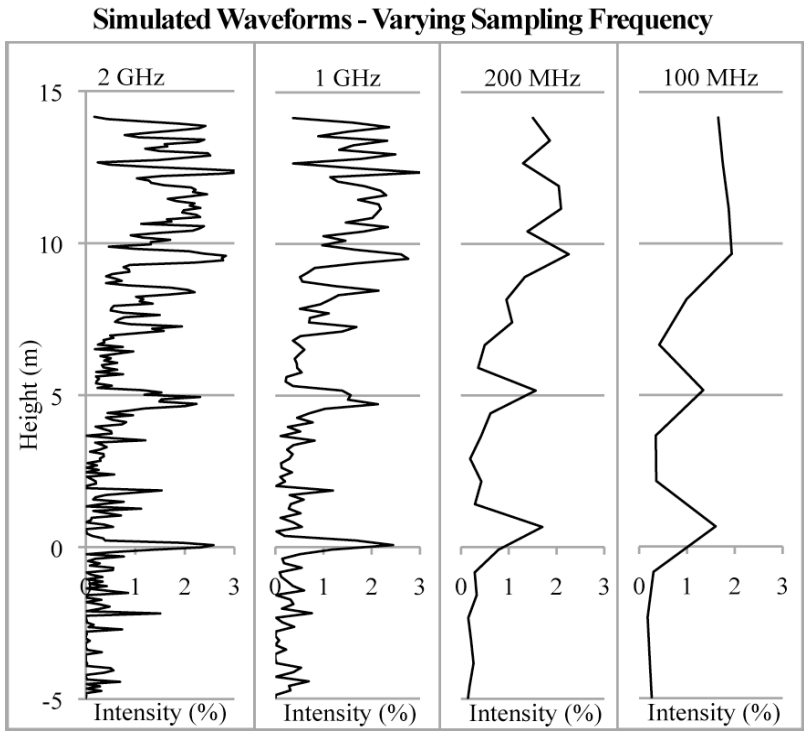


Figure 9. Comparison of waveforms recorded using varying LIDAR system sampling frequencies.

2.2 Test Case – LIDAR Interaction with a Leaf Surface

In this test case, the LIDAR interacts only with a leaf plate. The purpose of this test is to illustrate the capacity of the model to accurately simulate leaf radiometric properties. A leaf plate is simulated in the scene, with radiometric properties as determined by PROSPECT. There are no other materials in the scene, so any light that is transmitted through the leaf continues to travel out of the scene and is lost. Only the light that is reflected from the surface of the leaf is returned to the sensor. In Figure 10, the leaf reflectance and transmittance spectra from PROSPECT are plotted using solid lines; the results from the LIDAR simulation are plotted as symbols. There is excellent correlation between the two.

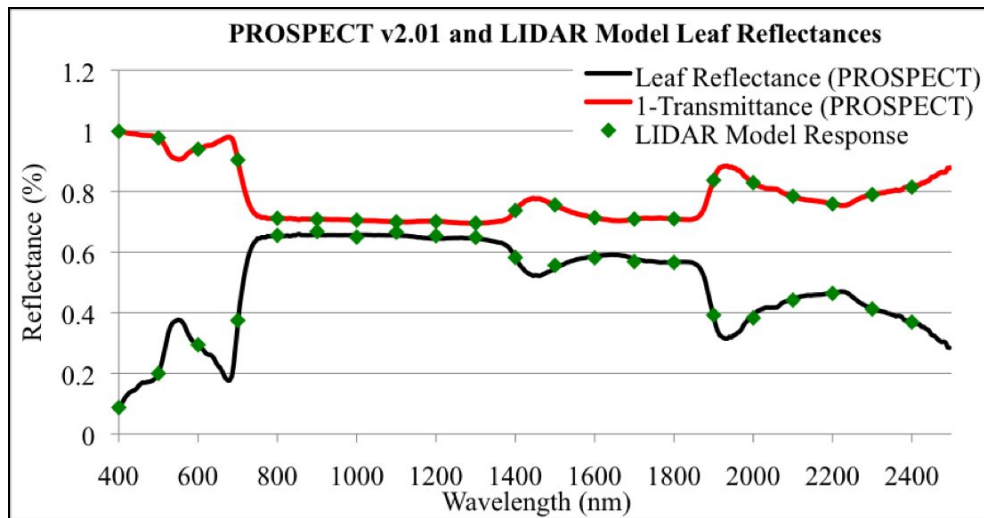


Figure 10. PROSPECT and LIDAR simulation model reflectance and transmittance spectra.

2.3 Test Case – Varying LIDAR Wavelength

In this test case, a leaf plate is simulated 1 m above a ground surface. Both the leaf and the ground are modeled as having Lambertian surface properties (Figure 11). Three laser wavelengths are examined – 532, 1064 and 1550 nm. The radiometric properties of the ground and leaf plate at these points is shown in Table 4.

Table 4. Material radiometric properties at various wavelengths

	532 nm	1064 nm	1550 nm
Leaf Plate - Reflectance, Transmittance, Absorbance	36%, 8%, 56%	66%, 30%, 4%	57%, 27%, 16%
Ground- Reflectance, Transmittance, Absorbance	10%, 0%, 90%	75%, 0%, 25%	45%, 0%, 55%

At 532 nm, the peak due to returns from the ground is minimal. Leaves at 532 nm absorb 56% of the energy incident upon them. In this simulation, the LIDAR pulse travels through the leaf plate twice – once on the way down, and again on the way back to the sensor. With 56% of the energy being absorbed by the leaf plate, the ground underneath the leaf plate is barely detected.

In the waveforms created by the 532 and 1550 nm LIDAR, there appear to be at multiple overlapping waveforms. This is due to the absorbance of the leaf plate. For the 532 nm LIDAR waveform, the most intense peak is 56% higher than the next less intense peak. For the 1550 nm LIDAR waveform, successive peaks decrease in intensity by 16%. Because these peaks occur at the same heights, this implies that energy must be interacting ‘within’ the leaf plate, rather than travelling to the ground and back. The LIDAR pulse hits the leaf plate, a portion of the energy is absorbed, and then the remaining energy is reflected back to the sensor. The illustration in Figure 12 is created from all of the individual points

returned to the sensor. In this simulation, each model step represents 0.1 ns, or a 10 GHz sampling frequency. The ‘multiple peaks’ artifact is masked by the sampling the waveform at any frequency less than 10 GHz.

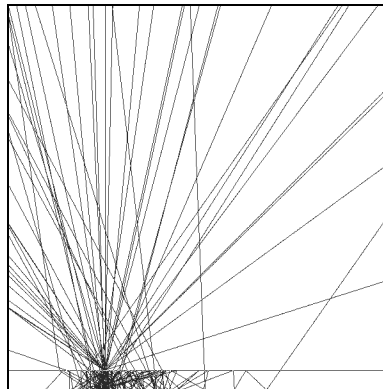


Figure 11. Interaction of first pulse of LIDAR energy for a Lambertian leaf ‘plate’ over a Lambertian ground surface.

As shown in Figure 12, the reflectance of the ground determines has a large impact on the strength of the ground return peak.

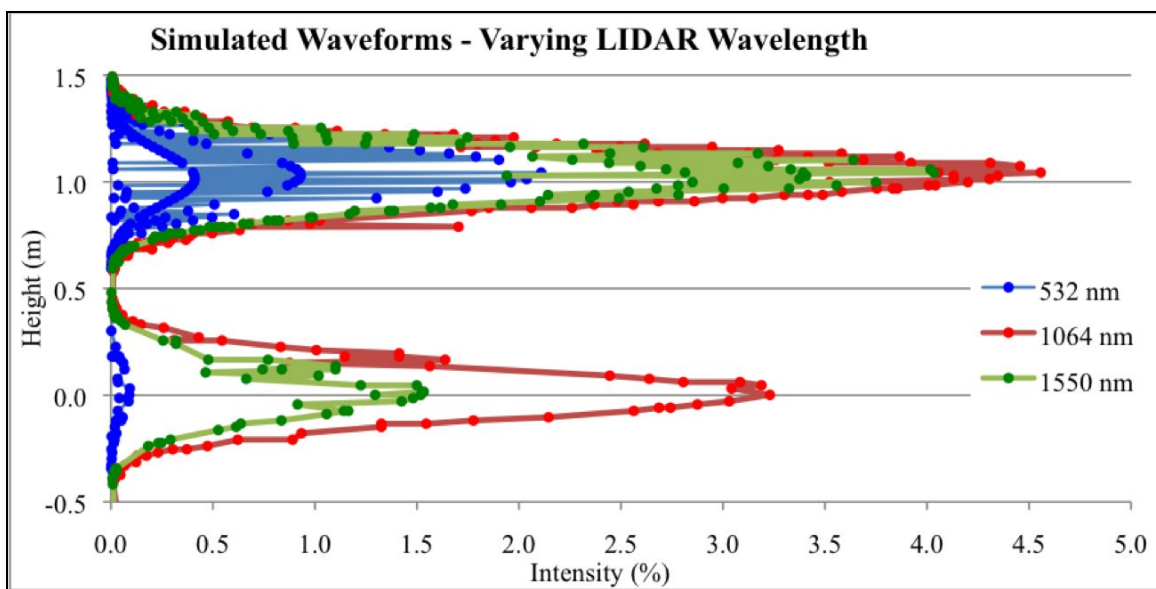


Figure 12. The simulated waveforms for a leaf plate over a ground surface. The LIDAR wavelength is varied from 532 to 1064 nm.

2.4 Test Case – Varying LIDAR Pulse Length

In this test case, the length of the LIDAR pulse is varied from 2 to 10 ns. This simulation has a leaf plate situated 0.24 m above the ground, with both the leaf and the ground modeled as Lambertian scattering surfaces. The purpose of this test is to demonstrate the affect of pulse length on the temporal resolution of the waveform. Figure 13 shows the transmitted LIDAR pulses, and Figure 14 shows the resulting waveforms.

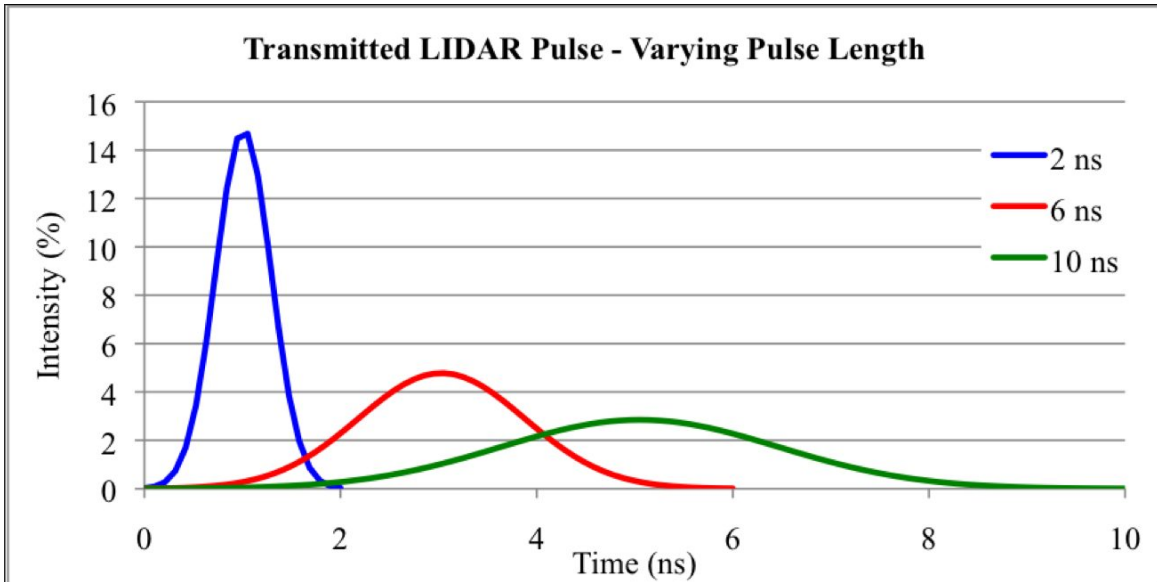


Figure 13. Transmitted LIDAR pulses of varying lengths. The pulse length varies from 6 to 14 ns.

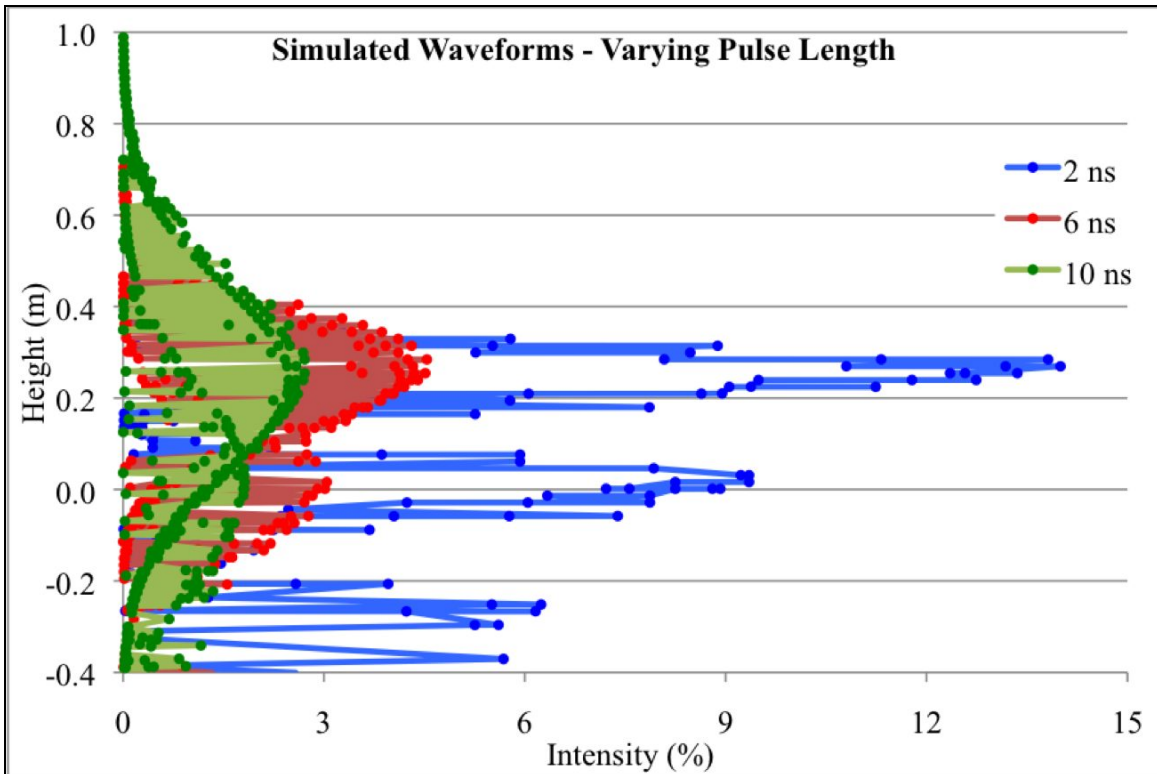


Figure 14. Simulated LIDAR waveforms for a Lambertian leaf plate above a Lambertian ground surface. The LIDAR pulse length varies from 6 to 14 ns.

This test case illustrates the effect of the LIDAR pulse length on the created waveform. Using a very short 2 ns LIDAR pulse, two separate peaks are distinguishable. With longer LIDAR pulses, the returns from the leaf plate and from the ground overlap, and distinguishing the two peaks in the overall waveform becomes more difficult. In general, a shorter LIDAR pulse yields a finer temporal resolution. As the length of the LIDAR pulse increases, the ability to distinguish objects at similar heights will decrease.

3. CONCLUSIONS AND FUTURE WORK

The model presented here shows the capability of simulating full-waveform LIDAR under a wide variety of parameters, which enables the analysis of the factors affecting waveform shape.

The results of the simulation need to be compared to real LIDAR data, and any differences addressed. Any model depends upon simplifying assumptions, and the validity of these assumptions needs to be verified.

Once the model has been verified, more complex scenes can be simulated and the results used to assist in the development of waveform processing algorithms.

REFERENCES

- [1] Baltsavias, E., "Airborne laser scanning: existing systems and firms and other resources," *ISPRS Journal of Photogrammetry and Remote Sensing* 54, 164–198 (1999).
- [2] Baltsavias, E., "Airborne laser scanning: Basic relations and formulas," *ISPRS Journal of Photogrammetry and Remote Sensing* 54, 199–214 (1999).
- [3] Clark, R. N., Swayze, G. A., Gallagher, A. J., King, T. V. V., and Calvin, W. M., "The U. S. Geological Survey, Digital Spectral Library: Version 1: 0.2 to 3.0 microns, (U.S. Geological Survey Open File Report 93–592)," (1993) Retrieved from http://speclab.cr.usgs.gov/spectral.lib04/clark1993/spectral_lib.html.
- [4] Jacquemoud, S., and Baret, F., "PROSPECT: a model of leaf optical properties spectra," *Remote Sensing of Environment* 34, 75–91 (1990).
- [5] Kim, A., "Simulating Full-waveform LIDAR," Masters Thesis, Naval Postgraduate School, Monterey, California, (2009).
- [6] Mallet, C. and Bretar, F., "Full-waveform topographic lidar: State-of-the-art," *ISPRS Journal of Photogrammetry and Remote Sensing* 64, 1–16 (2009).
- [7] Measures, R. M., [Laser remote sensing: Fundamentals and applications (reprint ed.)], Krieger Publishing Company, Malabar, FL, (1992).
- [8] Prusinkiewicz, P. and Lindenmayer, A., [The Algorithmic Beauty of Plants], Springer-Verlag, New York, (2004).
- [9] Shan, J. & Toth, C., [Topographic Laser Ranging and Scanning], CRC Press, Boca Raton, FL, (2009).